sign," Application Note 95, Sept. 1968.
[7] C. A. Desoer and E. S. Kuh, *Basic Circuit Theory*, vol. 2. New York: McGraw-Hill, 1967.
[8] W. Thommen and M. J. O. Strutt, "Noise figure of UHF Transistors," *IEEE Trans. Electron Devices*, vol. ED-12, Sept. 1965, pp. 499–500.
[9] W. Thommen, "Contribution to the signal- and noise equivalent circuit of UHF bipolar transistors" (in German), thesis 3658, Swiss Fed. Inst. Tech., 1965, Zurich, Switzerland.
[10] W. Beachtold and M. J. O. Strutt, "Noise in microwave transistors," *IEEE Trans. Microwave Theory Tech.*, vol. MTT-16, Sept. 1968, pp. 578–585.
[11] K. Hartmann, W. Kotyczka, and M. J. O. Strutt, "Equivalent networks for three different microwave bipolar transistor packages in the 2–10 GHz range," *Electron. Lett.*, no. 18, Sept. 1971, pp. 510–511.

Cavity Perturbation Techniques for Measurement of the Microwave Conductivity and Dielectric Constant of a Bulk Semiconductor Material

ISMAIL I. ELDUMIATI, MEMBER, IEEE, AND GEORGE I. HADDAD, SENIOR MEMBER, IEEE

Abstract—**Cavity perturbation techniques offer a very sensitive and highly versatile means for studying the complex microwave conductivity of a bulk material. A knowledge of the cavity coupling factor in the absence of perturbation, together with the change in the reflected power and the cavity resonance frequency shift, are adequate for the determination of the material properties. This eliminates the need to determine the Q-factor change with perturbation which may lead to appreciable error, especially in the presence of mismatch loss. The measurement accuracy can also be improved by a proper choice of the cavity coupling factor prior to the perturbation.**

I. Introduction

THE COMPLEX microwave conductivity of a semiconductor material has been measured using two different methods. In the first one a semiconductor slab completely fills a waveguide section and measurements are made to determine the complex reflection or transmission coefficients. This method has been reported by many authors [1]–[3] and has been reviewed recently by Datta and Nag [4]. The accuracy achieved with the reflection method is not very precise, especially with high-conductivity materials, since the VSWR to be measured is very high (nearly 20 dB) and the phase-angle is very small. On the other hand, when this method is used in a transmission mode, the accuracy is degraded further due to available commercial standards for attenuators and phase shifters. The fact that the sample should completely fill the transverse cross section of the waveguide poses two serious problems. First, in many cases it is very hard to get large enough samples to fill the waveguide cross section; this problem becomes more serious when the sample is a single crystal. Second, there is always a small air gap between the sample and waveguide walls, even with tight fitting, and this effect was shown to give erroneous results [5]. Recently, Holm [6] suggested a mode transducer to overcome this "gap effect." Holm's idea takes advantage of the fact that the contact problem is important when the electric field is normal to the sample's surface, and by converting the TE_{10} mode of the rectangular guide into a TE_{10} mode of a circular guide the electric field is tangential to the surface of the sample at the boundary. This scheme may be difficult to realize with a brittle material like InSb.

The second method for measuring the microwave conductivity is by using cavity perturbation techniques [7]–[10]. The material parameters are measured by determining the Q-factor change and the resonant frequency shift of a resonant cavity by inserting the sample in the region of maximum electric field. The strong interaction between the fields in the cavity and the sample makes this method very suitable for the measurement of small changes in the material properties as a result of external perturbations. If the sample is placed under the central post of a reentrant cavity with a high Q-factor, and the size of the sample is chosen such that the energy stored within the sample is much smaller than the energy stored in the cavity, it can be shown that the change in the material parameters as a result of perturbing the sample can be related to the cavity

Manuscript received January 28, 1971; revised May 28, 1971. This work was supported by the National Aeronautics and Space Administration under Grant NGL 23-005-183.

I. I. Eldumiati is with Sensors, Inc., Ann Arbor, Mich.
G. I. Haddad is with the Electron Physics Laboratory, Department of Electrical Engineering, University of Michigan, Ann Arbor, Mich. 48104.

resonant frequency shift and its Q-factor change as follows [11]:

$$\frac{f-f_0}{f_0}+\frac{1}{2Q_L}\left(\frac{1}{Q_L}-\frac{1}{Q_{L0}}\right) = \frac{\frac{\sigma}{(2\pi f)^2}(\sigma_0-\sigma)+\kappa_0^2\epsilon_r(\epsilon_{r0}-\epsilon_r)}{\kappa_0^2\epsilon_r^2+(\sigma/2\pi f)^2}(\eta) \quad (1)$$

and

$$\frac{1}{Q_L}-\frac{1}{Q_{L0}} = \frac{\sigma\epsilon_{r0}-\sigma_0\epsilon_r}{\kappa_0^2\epsilon_r^2+(\sigma/2\pi f)^2}\left(\frac{\kappa_0\eta}{2\pi f}\right) \quad (2)$$

where

$$\eta = \frac{1}{2}\frac{\int_{V_s}|E_0|^2dV}{\int_{V_c}|E_0|^2dV}$$

σ is the material conductivity, ϵ_r is its relative dielectric constant, κ_0 is the permittivity of free space, Q_L and f are the loaded Q-factor and resonant frequency of the cavity, and V_s and V_c are the volumes of the sample and the cavity, respectively. The subscript 0 indicates quantities in the absence of perturbation.

However, for samples of interest and at a frequency of 10 GHz, $\kappa_0^2\epsilon_r \gg \sigma/(2\pi f)^2$; also, it is quite reasonable to neglect $(1/2)(1/Q_L)[1/Q_L-1/Q_{L0}]$ with respect to $(f-f_0)/f_0$, which simplifies (1) and (2) to the following form:

$$\frac{\epsilon_r-\epsilon_{r0}}{\epsilon_r} = -\frac{f-f_0}{\eta f_0} \quad (3)$$

and

$$(\sigma-\sigma_0)+\frac{\sigma(f-f_0)}{\eta f_0} = \frac{\epsilon_r\kappa_0\omega}{\eta}\left(\frac{1}{Q_L}-\frac{1}{Q_{L0}}\right). \quad (4)$$

Equations (3) and (4) relate the change in the conductivity and dielectric constant of the sample to the experimentally measurable quantities. The parameter η depends on the geometry of the sample and the cavity. This parameter can be determined either experimentally by using a sample with known parameters, or theoretically by studying the fields within the cavity. Equation (3) can be used to study the change in the dielectric constant as a result of perturbing the sample. Using (4) to study the change in the material conductivity could result in erroneous results due to the fact that the values of Q_L and Q_{L0} are very close to each other. This paper suggests an alternative method using power measurement. In the following analysis it will be shown that a knowledge of the coupling factor in the absence of perturbation together with the change in the reflected power and resonance frequency shift as a result of the perturbation are adequate for the determination of the material conductivity. This eliminates the need to determine the Q-factor change as a function of the perturbation which might lead to appreciable error in the presence of mismatch loss. The method offers an accurate way to measure changes in the material conductivity as a result of perturbing the sample (due to temperature variation, or electric or magnetic fields).

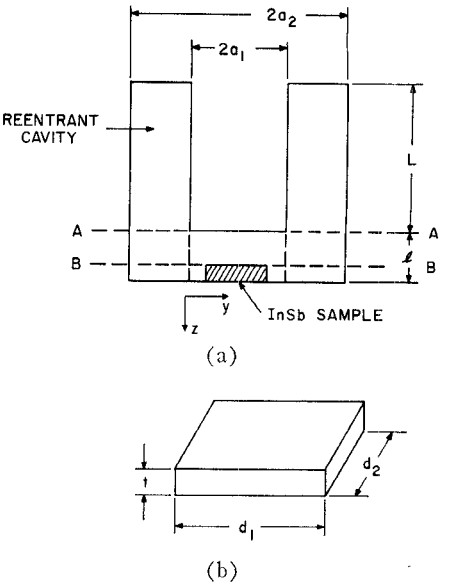

Fig. 1. Orientation and dimensions of the cavity and sample. (a) Sample orientation within the cavity. (b) Sample dimensions.

II. Cavity Analysis

A. Equivalent Circuit of the Cavity Including the Sample

Fig. 1 shows the material orientation within the cavity together with the dimensions of the sample. Placing the sample under the central post of the reentrant cavity has the following advantages.

1) The electric field is maximum in this region, which results in a greater interaction between the sample and the signal.

2) The field is essentially uniform over the sample, which simplifies the analysis considerably. This holds for samples where the skin depth is larger than the sample dimension along the electric field, which is the case for the samples employed here.

The cavity is divided into two parts by the plane A–A. The section above this plane can be represented by a transmission line terminated in a short circuit. This part is equivalent to an RLC in shunt. The value of these elements (L_0, R_0, and C_0) are functions of the dimensions a_1, a_2, L, and the conductivity of the cavity walls. The section below plane A–A adds an extra shunt admittance Y which will depend on the parameters of the sample. It is fairly reasonable to assume that most

of the contribution of this section to Y comes from the region underneath the central post. With this in mind the admittance Y could be divided into three components.

1) A capacitance C_1 due to the air gap between the two planes A–A and B–B under the central post and is given by

$$C_1 = \frac{\kappa_0 \pi a_1^2}{l - t}. \tag{5}$$

2) An admittance Y_m due to the presence of the sample whose value is given in the Appendix.

3) A second capacitance C_2 due to the air gap under the plane B–B that is not occupied by the sample and is given by

$$C_2 = \frac{\kappa_0(\pi a_1^2 - d_1 d_2)}{t}. \tag{6}$$

The equivalent admittance of the cavity section below plane A–A is composed of that of C_1 in series with the shunt combination of C_2 and Y_m and is given by

$$Y = G_{\text{eff}} + j\omega C_{\text{eff}} \tag{7}$$

where

$$G_{\text{eff}} = \frac{G'}{\dfrac{G_m'^2}{\omega^2 C_1^2} + \left(1 + \dfrac{C'}{C_1}\right)^2} \tag{8}$$

$$C_{\text{eff}} = C_1 \frac{1 + \dfrac{\omega^2 C_1 C'}{G_m'^2}\left(1 + \dfrac{C'}{C_1}\right)}{1 + \dfrac{\omega^2 C_1^2}{G_m'^2}\left(1 + \dfrac{C'}{C_1}\right)^2}. \tag{9}$$

$C' = C_m' + C_2$, and both C_m' and G_m' are defined in (33) and (34) of the Appendix.

If the material is isotropic, both σ_{12} and ϵ_{12} become zero and the expressions for G_{eff} and C_{eff} become

$$G_{\text{eff}} = \frac{K_1 \sigma}{\dfrac{K_1^2 \sigma^2}{\omega^2 C_1^2} + \left(1 + \dfrac{C}{C_1}\right)^2} \tag{10}$$

and

$$C_{\text{eff}} = C_1 \frac{1 + \dfrac{\omega^2 C^2}{K_1^2 \sigma^2}\left(1 + \dfrac{C_1}{C}\right)}{1 + \dfrac{\omega^2 C^2}{K_1^2 \sigma^2}\left(1 + \dfrac{C_1}{C}\right)^2} \tag{11}$$

where $C = C_2 + K_1 \epsilon$. For most semiconductor samples both $(\omega C/K_1\sigma)^2$ and $(\omega C_1/K_1\sigma)^2$ are much greater than one. This reduces (10) and (11) to the following forms:

$$G_{\text{eff}} = K\sigma \tag{12}$$

and

$$C_{\text{eff}} = \frac{C_1 C}{C_1 + C} \tag{13}$$

where

$$K = [K_1/(1 + C/C_1)^2].$$

The change in the conductivity of the material will change the equivalent conductance of the test cavity and can be measured by monitoring the change in the power reflected from the cavity. On the other hand, the change in the dielectric constant of the material will in turn change C_{eff} and as a result the resonance frequency of the cavity will shift.

B. Conductivity Change

The dependence of the conductivity of the material on the change of the power reflected by the cavity is presented in this section. The circuit used for measurements is illustrated in Fig. 2. In this analysis the power is coupled to the cavity through a circulator and a lossy line with attenuation α. For simplicity the circulator is assumed to be matched to both the line and the detector; however, if any mismatch loss is present it can be easily taken into account. The various measurable power levels can be defined as follows.

- P_0 Power available from the source, which is the power delivered to a matched load through a lossless coupling.
- P_r Power reflected from the cavity.
- P_D $= \alpha P_r$ is the detected power.

The change in the detected power ΔP_D due to the introduction of perturbation can be expressed as

$$\Delta P_D = -\alpha(P_D - P_{D0}) \tag{14}$$

where the subscript zero denotes quantities in the absence of perturbation.

The change in the detected power ΔP_D as a result of a change in the material conductivity from σ_0 to σ can be obtained from the cavity equivalent circuit at resonance shown in Fig. 3 and is expressed as follows:

$$\frac{\Delta P_D}{P_D} = -4\alpha\left(\frac{(1 + x)\beta_0}{(1 + x + \beta_0)^2} - \frac{\beta_0}{(1 + \beta_0)^2}\right) \tag{15}$$

where β_0 is the coupling factor with no perturbation and is given by

$$\beta_0 = Y_0/(K\sigma_0 + G_0) \tag{16}$$

$$x = F(\Delta\sigma/\sigma_0)$$

and

$$F = K\sigma_0/(G_0 + K\sigma_0). \tag{17}$$

It is seen that once P_0 and β_0 are known it is a straightforward process to determine the change in the

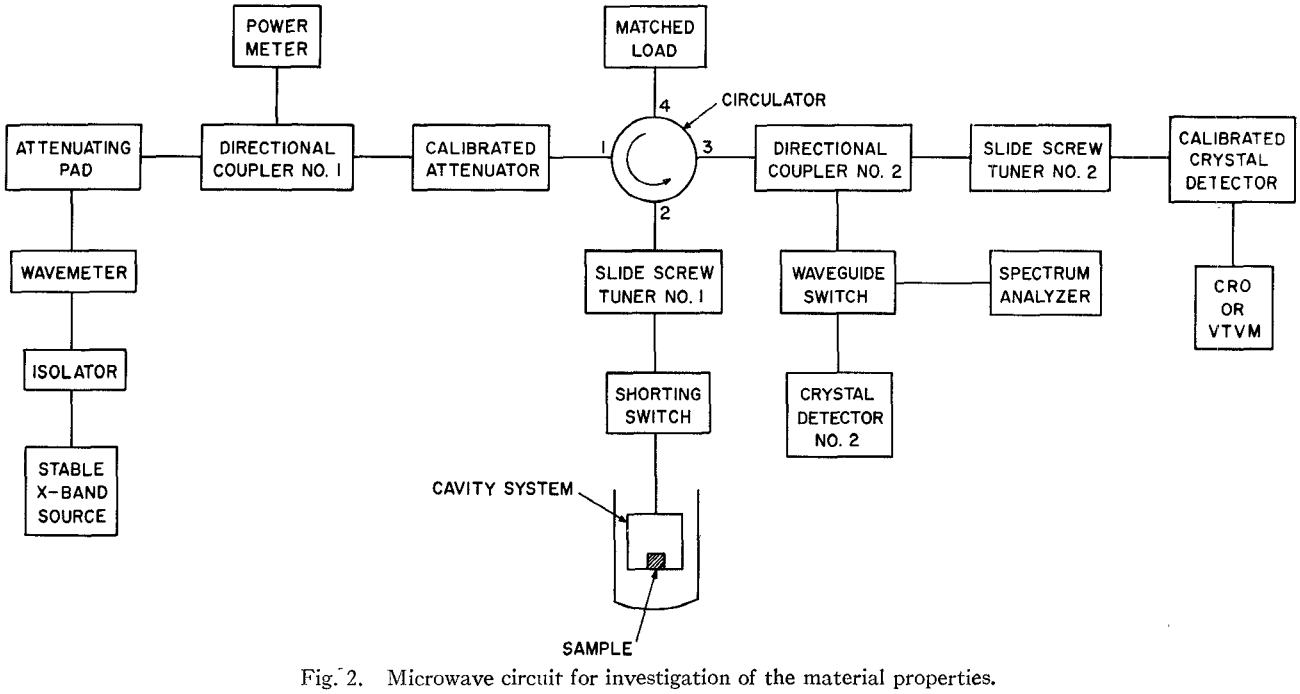

Fig. 2. Microwave circuit for investigation of the material properties.

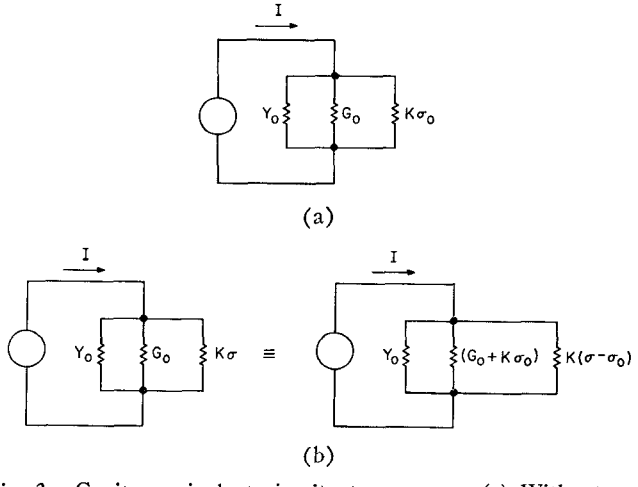

Fig. 3. Cavity equivalent circuit at resonance. (a) Without perturbation. (b) With perturbation.

material conductivity from measurement of the corresponding change in the detected power. Both β_0 and ΔP can be measured to a much higher degree of accuracy when compared to the Q-factor, especially in the presence of mismatch and insertion loss. However, there exists an optimum coupling factor which results in the largest value of $\Delta P_D/P_0$ for a certain value of x. The knowledge of such a coupling factor will improve the accuracy of the experimental results. To determine this optimum coupling factor, the first derivative with respect to β_0 of the left-hand side of (15) is equated to zero, which results in

$$[\beta_{op}^4 - (x+2)\beta_{op}^3 - 6(x+1)\beta_{op}^2 - (x+1)(x+2)\beta_{op} + (x+1)^2]x = 0 \quad (18)$$

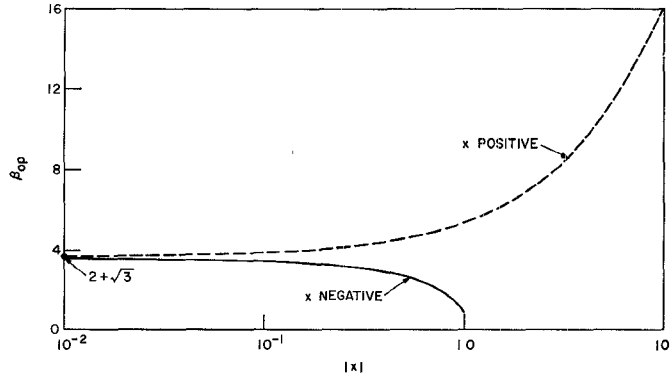

Fig. 4. Optimum coupling factor for overcoupled cavities.

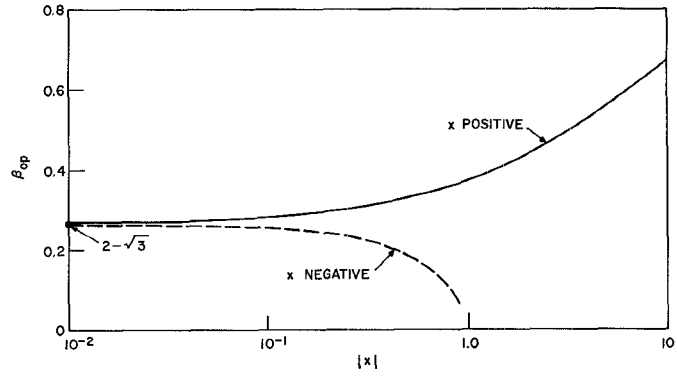

Fig. 5. Optimum coupling factor for undercoupled cavities.

where β_{op} is the optimum coupling factor. Figs. 4 and 5 give plots of the optimum coupling factor versus x for overcoupled and undercoupled cavities, respectively. It is worthwhile to investigate the case when $x \ll 1$ in order

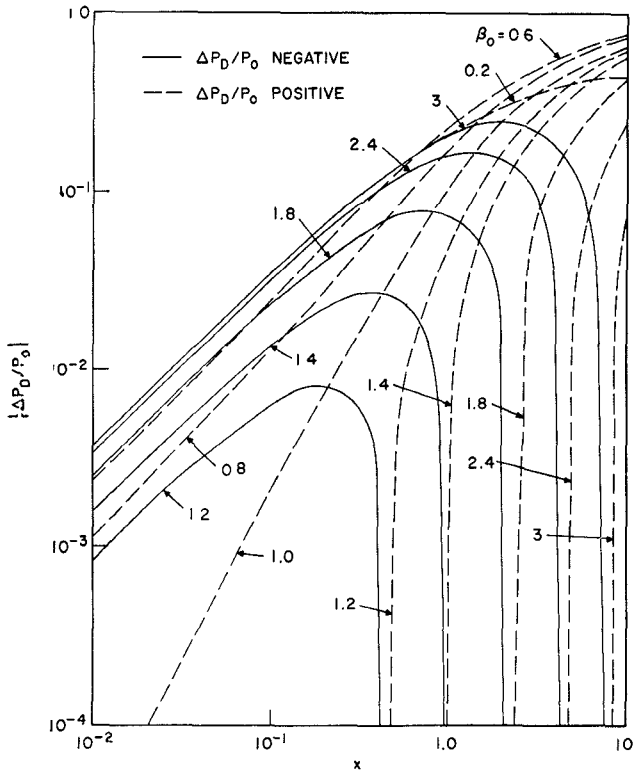

Fig. 6. The relative change in the detected power versus positive values of x. ($\alpha=1$.)

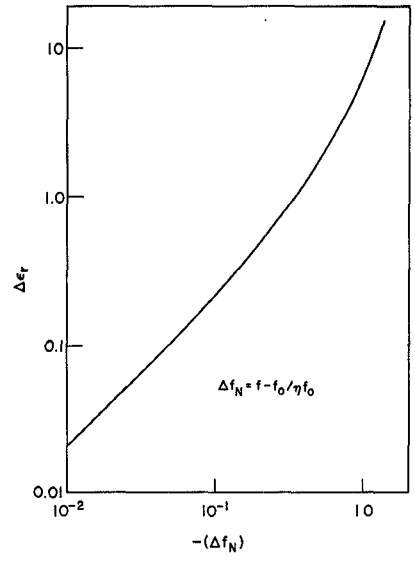

Fig. 7. Change in the relative dielectric constant of the sample versus Δf_N.

to get more insight from these figures. In such a case, (18) reduces to the following,

$$\beta_{op}^4 - 2\beta_{op}^3 - 6\beta_{op}^2 - 2\beta_{op} + 1 = 0. \quad (19)$$

The four roots of (19) are -1, -1, $(2+\sqrt{3})$, and $(2-\sqrt{3})$. The two roots having the value of -1 have no physical significance and will be disregarded. The remaining two roots indicate that either an undercoupled or overcoupled cavity can be designed for optimum test conditions. The criterion to choose between an overcoupled or an undercoupled cavity is determined by the fact that the cavity should not change from one kind of coupling to the other as a result of the perturbation. This requirement will cause the detected power to be either monotonically increasing or decreasing as a result of the introduction of perturbation. As a result any confusion due to a change in the kind of coupling is totally eliminated. A study of the change in the cavity coupling factor as a result of the perturbation for various values of β_0 shows that if the perturbation increases the conductivity of the material under test (x is positive), the cavity should be undercoupled, and the opposite is true. Therefore, the solid lines in Figs. 4 and 5 will serve to give the optimum coupling factor according to the anticipated change in the conductivity of the material.

C. Calibration of the Cavity System

In order to study the change in the material conductivity and dielectric constant as a result of the perturbation the parameters η and F should be determined. Moreover, it is necessary to investigate the dependence of these parameters together with β_0 on the perturbation.

It should be emphasized that the method can be generalized very easily for large changes in ϵ_r and σ through numerical analysis. The programming is done through iterative steps where each step corresponds to a very small change in σ or ϵ_r. The results obtained after each iteration serve as initial conditions for the subsequent step. Typical results for this analysis are shown in Figs. 6 and 7.

The geometrical factor η can be determined by studying the field configuration within the cavity system. However, this is a very lengthy and involved process, especially if higher order modes are excited. This factor can be determined experimentally by studying the frequency shift due to samples having a known dielectric constant and having the same dimensions as the sample under test. The resonance frequency shift from that of the empty cavity ($\epsilon_r=1$) can be used in conjunction with Fig. 7 to determine η.

It can be shown that F can be determined by measuring the coupling factor of the empty cavity and that with the sample present at no perturbation.

From (16) G_0/σ_0 is given by

$$G_0/\sigma_0 = K_0\beta_0/(\beta_{00} - \beta_0) \quad (20)$$

where β_{00} is the coupling factor of the empty cavity.

Substituting (20) into (17) yields

$$F = \frac{\beta_{00} - \beta_0}{\beta_{00} - \beta_0\left(1 - \dfrac{K_0}{K}\right)} \quad (21)$$

where K_0 is the value of K in the absence of perturbation. If the resonance frequency shift as a result of the

TABLE I
THE RELATIVE CHANGE OF THE DETECTED POWER AT THE CRITICAL POINTS

Incident Power (dBm)	β_0	Measured $\lvert\Delta P/P_0\rvert$	Calculated $\lvert\Delta P/P_0\rvert$
−2	0.64	48×10^{-3}	48.16×10^{-3}
−4	0.64	49.5×10^{-3}	48.16×10^{-3}
−4	0.33	248×10^{-3}	253.8×10^{-3}
−4	1.5	37.5×10^{-3}	39.8×10^{-3}
−11	0.6	54.5×10^{-3}	62.5×10^{-3}

perturbation is negligible, then $K = K_0$ and $F = F_0$, and is given by

$$F_0 = \left(1 - \frac{\beta_0}{\beta_{00}}\right). \tag{22}$$

III. SUMMARY AND CONCLUSIONS

A measurement procedure for determining the microwave properties of a semiconductor material using cavity perturbation techniques has been presented. The method is different from the conventional approach, which relies on the Q-factor measurements. It has been shown that the change in the material conductivity as a result of some perturbation can be measured by measuring the cavity coupling factor prior to the perturbation and the change in the reflected power from the cavity as a result of the perturbation. Both parameters can be measured to within 1-percent accuracy. In addition, the effect of the coupling factor toward improving the accuracy has been determined. The approach is very valuable when the change in the material properties is very small. The method has been checked experimentally by perturbing an InSb sample through application of a magnetic field, and checking the theoretical and experimental values for the change in the reflected power required to bring the cavity to critical coupling. The results are summarized in Table I. It is seen from these results that theory and experiment are in excellent agreement, which justifies the previous approach.

APPENDIX

EQUIVALENT CIRCUIT OF A SEMICONDUCTOR MATERIAL IN A REENTRANT CAVITY

The equivalent circuit of the sample placed under the central post of the cavity, as shown in Fig. 1, will be derived here. The sample will carry both conduction and displacement currents, i.e.,

$$J = \bar{\sigma}\boldsymbol{E} + \frac{\partial \boldsymbol{D}}{\partial t} \tag{23}$$

where $\boldsymbol{D}$ is the electric-displacement vector, $\boldsymbol{E}$ is the electric-field intensity, and $\bar{\sigma}$ is the conductivity tensor. Since the microwave field due to the dominant TEM mode is parallel to the x axis and varies as $e^{j\omega t}$, (23) can be written as

$$J = \bar{\sigma}\boldsymbol{E} + j\omega\epsilon\boldsymbol{E}. \tag{24}$$

The conductivity tensor of a material in the presence of a magnetic field along the z axis can be written as

$$\bar{\sigma} = \begin{bmatrix} \sigma_{xx} & \sigma_{xy} & 0 \\ \sigma_{yx} & \sigma_{yy} & 0 \\ 0 & 0 & \sigma_{zz} \end{bmatrix}. \tag{25}$$

Therefore, by substituting (25) into (23), the x- and y-components of the current density can be written as follows

$$J_x = (\sigma_{xx} + j\omega\epsilon_{xx})E_x + (\sigma_{yx} + j\omega\epsilon_{yx})E_y \tag{26}$$

and

$$J_y = (\sigma_{xy}E_x + j\omega\epsilon_{xy})E_x + (\sigma_{yy} + j\omega\epsilon_{yy})E_y. \tag{27}$$

The continuity of current at the surface of the sample normal to the y axis implies that the displacement current outside the sample should be equal to the total current within the sample. And since the electric field is uniform and along the x axis, $J_y = 0$. Therefore,

$$E_y = -\frac{\sigma_{xy} + j\omega\epsilon_{xy}}{\sigma_{yy} + j\omega\epsilon_{yy}} E_x. \tag{28}$$

Substituting (28) into (26) yields,

$$J_x = \left((\sigma_{xx} + j\omega\epsilon_{xx}) - \frac{(\sigma_{xy} + j\omega\epsilon_{xy})(\sigma_{yx} + j\omega\epsilon_{yx})}{\sigma_{yy} + j\omega\epsilon_{yy}}\right) E_x. \tag{29}$$

Therefore, the equivalent admittance of a sample of thickness t and an area A follows immediately from (29),

$$Y_m = K_1(\sigma_{xx} + j\omega\epsilon_{xx}) + Y_{\text{ani}} \tag{30}$$

where $K_1 = d_1 d_2/t$, Y_m is the equivalent conductance of the material, and Y_{ani} is the contribution to Y_m due to the anisotropy of the material, and is given by

$$Y_{\text{ani}} = -\frac{(\sigma_{xy} + j\omega\epsilon_{xy})(\sigma_{yx} + j\omega\epsilon_{yx})}{\sigma_{yy} + j\omega\epsilon_{yy}} K_1. \tag{31}$$

However, it has been shown that [12] $\sigma_{xy} = -\sigma_{yx}$ and $\epsilon_{xy} = -\epsilon_{yx}$, and thus Y_m reduces to

$$Y_m = G_m' + j\omega C_m' \tag{32}$$

where

$$G_m' = K_1\left(\sigma_{xx} + \frac{\sigma_{12}^2}{\sigma_{yy}^2 + \omega^2\epsilon_{yy}^2}\sigma_{yy}\right) \tag{33}$$

and

$$C_m' = K_1\left(\epsilon_{xx} - \epsilon_{yy}\frac{\sigma_{12}^2}{\sigma_{yy}^2 + \omega^2\epsilon_{yy}^2}\right) \tag{34}$$

where $\epsilon_{xy} = -\epsilon_{yx} = \epsilon_{12}$ and $\sigma_{xy} = -\sigma_{yx} = \sigma_{12}$. If σ_{12} is much greater than $\omega\epsilon_{12}$, then the equivalent admittance of the

sample becomes

$$Y_m = K_1\left(\sigma_{xx} + j\omega\epsilon_{xx} + \frac{\sigma_{12}^2}{\sigma_{yy} + j\omega\epsilon_{yy}}\right). \quad (35)$$

On the other hand, if the material is isotropic, the expression for the equivalent admittance of the sample becomes

$$(Y_m)_{\text{iso}} = K_1(\sigma + j\omega\epsilon). \quad (36)$$

References

[1] K. S. Champlin, J. D. Holm, and G. H. Glover, "Electrodeless determination of semiconductor conductivity from TE_{01}°-mode reflectivity," *J. Appl. Phys.*, vol. 38, pp. 96–98, Jan. 1967.

[2] F. A. D'Altroy and H. Y. Fan, "Microwave transmission in p-type germanium," *Phys. Rev.*, vol. 94, pp. 1415–1416, June 1954.

[3] H. Jacobs, F. A. Brand, J. D. Meindl, S. Weitz, and R. Benjamin, "New microwave technique in the measurement of semiconductor phenomenon," in *IRE Int. Conv. Rec.*, vol. 10, pt. 3, pp. 30–42, Mar. 1962.

[4] A. N. Datta and B. R. Nag, "Techniques for the measurement of complex microwave conductivity and the associated errors," *IEEE Trans. Microwave Theory Tech.*, vol. MTT-18, pp. 162–166, Mar. 1970.

[5] K. S. Champlin and G. H. Glover, " 'Gap effect' in measurement of large permittivities," *IEEE Trans. Microwave Theory Tech.* (Corresp.), vol. MTT-14, pp. 397–398, Aug. 1966.

[6] J. D. Holm, "Microwave conductivity of silicon and germanium," Ph.D. dissertation, the University of Minnesota, Minneapolis, 1967.

[7] H. M. Altschuler, "Dielectric constant," in *Handbook of Microwave Measurements*, vol. II, M. Sucher and J. Fox, Eds. Brooklyn, N. Y.: Polytechnic Press, 1963, pp. 495–590.

[8] H. R. G. Casimir, "On the theory of electromagnetic waves in resonant cavities," *Phillips Res. Reps.*, vol. 6, 1951.

[9] E. L. Ginzton, *Microwave Measurements*. New York: McGraw-Hill, 1957.

[10] R. A. Waldron, "Perturbation theory of resonant cavities," *Proc. Inst. Elec. Eng.*, vol. 107C, pp. 272–274, Sept. 1960.

[11] I. I. Eldumiati, "Bulk semiconductor materials for millimeter- and submillimeter-wave detection," Electron Physics Laboratory, the University of Michigan, Ann Arbor, Tech. Rep. 118, Grant NGL 23-005-183, Dec. 1970.

[12] S. R. De Groot and P. Mazur, "Extension of Onsager's theory of reciprocal relations," *Phys. Rev.*, vol. 94, pp. 218–226, Apr. 1954.

Traveling-Wave Coherent Light-Phase Modulator

M. EZZAT EL-SHANDWILY, MEMBER, IEEE, AND SAID M. EL-DINARY

Abstract—**The use of a rectangular waveguide partially loaded with electrooptic material as a laser beam phase modulator is analyzed theoretically. The characteristic equation, fields, power, and attenuation are obtained in terms of normalized parameters. Design procedure of the modulator is given with particular reference to KDP.**

I. Introduction

THE USE OF electrooptic (EO) materials for amplitude or phase modulation of a coherent light beam has been analyzed by several authors [1]. For a traveling-wave modulator, a waveguide partially filled with the EO crystal is usually used to support the modulating signal. Kaminow and Liu [2] analyzed the propagation characteristics of a parallel plate guide partially loaded with KDP crystal. In their analysis, TEM fields are used to produce phase modulation of the coherent beam. They found that for practical KDP crystal dimensions, 3 GHz is the highest frequency for broad-band operation for the collinear geometry. Higher order modes have not been considered. Peters [3] demonstrated experimentally the operation of a traveling-wave coherent light-phase modulator. The structure used was similar to that analyzed theoretically by Kaminow and Liu [2]. A modulation index of unity was obtained with a modulating power of 12 W. Chen and Lee [4] analyzed the propagation characteristics of a cylindrical waveguide partially filled with a cylindrical dielectric light modulation material. They considered only modes with no angular variation. Their analysis reveals that for TM mode propagation there is a nondispersive region which is suitable for broad-band modulation.

Recently, Putz [5] described an experimental microwave-light modulator, using a ring-phase traveling-wave circuit, with KDP crystals filling the space inside the rings. The KDP crystal is used in the longitudinal mode, i.e., with the light beam along the optic axis. The modulator uses 10 W of input power to produce AM modulation at a modulation depth of 40 percent with 10-percent bandwidth. However, for phase modulation it gives only a modulation index of 0.2 rad. Vartanian *et al.* [6] investigated the propagation characteristics of TE_{n0} modes in dielectric loaded rectangular waveguide. Our work is concerned with the same structure for use as a laser beam phase modulator.

In Section II, we give a brief description of the phase change in a laser beam traveling through an EO crystal in the presence of an RF field. Section III treats the problem of electromagnetic wave propagation through

Manuscript received February 1, 1971; revised March 15, 1971.

M. E. El-Shandwily is with the National Research Center, Electrical and Electronic Research Laboratory, Sh. El-Tahrir, Dokki-Cairo, Egypt.

S. M. El-Dinary is with the Atomic Energy Establishment, Cairo, Egypt.